Available online at www.sciencedirect.com
ScienceDirect
Ceramics International 38S (2012) S225–S228
CERAMICS INTERNATIONAL
www.elsevier.com/locate/ceramint

Preparation of PZT-based piezoceramics with transgranular fracture mode

Rui-fang Yue [a], Wen-ze He [a], Fei-fei An [a], Jian Yu [a,*], Guo-chao Chen [b]

[a] Functional Materials Research Laboratory, Tongji University, Shanghai, 200092, China
[b] Wuxi Zhongke Ultrasonic Technology Ltd, 8 Chunyu Road, Wuxi, 214001, China

Available online 4 May 2011

Abstract

In this paper, the effect of various doping and substitution elements on the mechanical fracture of perovskite-type $(Pb_{0.95}Sr_{0.05})(Zr_{0.52}Ti_{0.48})O_3$–$Pb(Mn_{1/3}Sb_{2/3})O_3$–$Pb(Mn_{1/3}Nb_{2/3})O_3$ and $(Pb_{0.95}Sr_{0.04})(Zr_{1-x}Ti_x)O_3$–$Pb(Mg_{1/3}Nb_{2/3})O_3$ ceramics was investigated. The predominant transgranular fracture mode was observed in the modified piezoceramics mentioned above and the ZnO, SnO_2 and SiO_2 as trace additives were found beneficial to enhance the mechanical bonding force of grain boundaries. The mechanism of transgranular fracture mode was understood by the diffusion of doping elements into the structural lattice of perovskite-type oxides, agreed with the experimental results of reduced tetragonality, dielectric constant and piezoelectric coefficient.

Keywords: A. Powders: solid state reaction; B. Electron microscopy; C. Piezoelectric properties; D. PZT

1. Introduction

Lead zirconate titanate (PZT) based ceramics are the most important piezoelectric functional materials and have been intensively and widely studied and practically applied in the sensors, actuators and transducers. It has been revealed that the piezoelectric properties are close associated with the mechanical properties, i.e. improved mechanical properties and enhanced piezoelectric properties [1]. From the results of fracture mechanics of ceramics, it is well known that, for polycrystalline piezoelectric ceramics, the mechanically weak grain boundary usually results in the intergranular fracture of ceramic patches and the crack path (intergranular, transgranular, or mixed) was observed depending on various microstructural factors such as the character of grain boundary, the grain size, the porosity [2–6]. In the past twenty years, various factors of sintering condition and sintering additive such as SiO_2, LiF, WO_3 have been found to set different influences on the fracture mode of piezoelectric ceramics, and when the fracture mode changed from intergranular to transgranular, the dielectric constant and piezoelectric constant d_{33} usually increased [7–13]. For example, a small amount of SiO_2 was found to improve the flexural strength, microhardness and dielectric constant of $Pb(Zr_{0.58}Fe_{0.20}Nb_{0.20}Ti_{0.02})_{0.994}U_{0.006}O_3$ ceramics while the fracture mode observed by SEM was essentially transgranular [8]. Adding MgO into PZT ceramics was also observed cause the PZT fracture mode gradually change from intergranular to transgranular [10].

Therefore, to obtain transgranular fracture mode via controlling microstructure with dopants and trace additives is substantially useful way to optimize piezoelectric and mechanical properties of PZT-based ceramics, in particular those piezoceramics for high power applications. Here, we presented attempts of controlling ceramic fracture mode through doping method and discussed the underlying mechanism.

2. Experimental procedures

Here, the high power piezoceramics with general formula of $(Pb_{0.95}Sr_{0.05})(Zr_{0.52}Ti_{0.48})O_3$–$Pb(Mn_{1/3}Sb_{2/3})O_3$–$Pb(Mn_{1/3}Nb_{2/3})O_3$ and high dielectric constant one of $(Pb_{0.95}Sr_{0.04})(Zr_{1-x}Ti_x)O_3$–$Pb(Mg_{1/3}Nb_{2/3})O_3$ with various doping elements were prepared with conventional electroceramic processing. Commercial PbO, $SrCO_3$, Sb_2O_3, MnO_2, Nb_2O_5, ZrO_2, TiO_2, NiO, SiO_2, ZnO and SnO_2 were used as the raw materials and weighted in accordance with the tentative formula. The stoichiometric mixtures were ground with ethanol

* Corresponding author. Tel.: +86 21 65980544; fax: +86 21 65985179.
E-mail address: jyu@tongji.edu.cn (J. Yu).

0272-8842/$36.00
doi:10.1016/j.ceramint.2011.04.088

and calcined at 800 °C for 5 h. The calcined powders were reground, granulated and uniaxially pressed into 10 mm green disks at 250 MPa and sintered in a close alumina crucible at temperature between 1280 and 1300 °C for 2 h with linear shrinkage rate above 12%. For electrical characterization, the ceramic pellets were polished, coated with silver paste and fired at 600 °C for 10 min, and subsequently poled under a DC electric field of 3–4 kV/mm in a silicon oil bath at 120 °C for 20 min.

The phase structure and lattice constants were examined by X-ray diffraction (XRD, D8, Bruker AXS Gmbh, German). The microstructure of fracture surface was observed by scanning electron microscopy (SEM, JSM EMP-800, Japan). After 24 h aging at room temperature, the dielectric constant and loss were measured with Agilent 4284A LCR meter, the piezoelectric constant measured with a quasistatic piezoelectric d_{33}-meter.

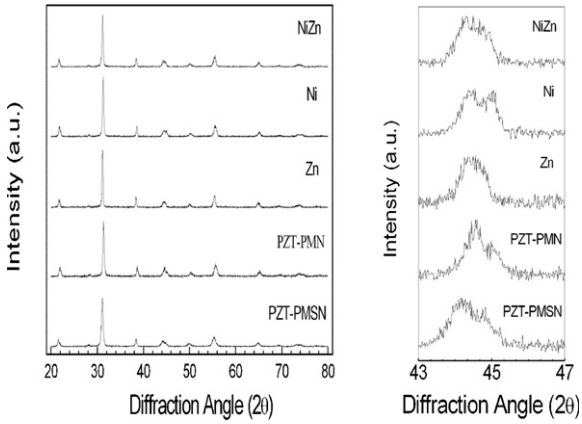

Fig. 1. XRD patterns for the modified PZT–PMSN, PZT–PMN, modified PZT–PMN–PZN (marked as Zn), PZT–PMN–PNN (marked as Ni), and modified PZT–PMN–PNN (marked as NiZn) ceramic samples.

3. Results and discussion

Fig. 1 presented the XRD patterns of the $0.95(Pb_{0.95}Sr_{0.05})(Zr_{0.52}Ti_{0.48})O_3$–$0.025Pb(Mn_{1/3}Sb_{2/3})O_3$–$0.025Pb(Mn_{1/3}Nb_{2/3})O_3$ + 1% ZnO + 0.5%SnO_2 (labeled as modified PZT–PMSN), $0.65(Pb_{0.95}Sr_{0.04})(Zr_{0.41}Ti_{0.59})O_3$–$0.35Pb(Mg_{1/3}Nb_{2/3})O_3$ + 1.5% SiO_2 (labeled as PZT–PMN), $0.72(Pb_{0.95}Sr_{0.04})(Zr_{0.45}Ti_{0.55})O_3$–$0.26Pb(Mg_{1/3}Nb_{2/3})O_3$–$0.02Pb(Zn_{1/3}Nb_{2/3})O_3$ + 1.5% SiO_2 + 1% ZnO + 0.5% SnO_2 (labeled as modified PZT–PMN–PZN), $0.72(Pb_{0.95}Sr_{0.04})(Zr_{0.45}Ti_{0.55})O_3$–$0.26Pb(Mg_{1/3}Nb_{2/3})O_3$–$0.02Pb(Ni_{1/3}Nb_{2/3})O_3$ + 1.5% SiO_2 (labeled as PZT–PMN–PNN), and $0.72(Pb_{0.95}Sr_{0.04})(Zr_{0.45}Ti_{0.55})O_3$–$0.26Pb(Mg_{1/3}Nb_{2/3})O_3$–$0.02Pb(Ni_{1/3}Nb_{2/3})O_3$ + 1.5% SiO_2 + 1% ZnO + 0.5% SnO_2 (labeled as modified PZT–PMN–PNN) (left) in the range of 20–80° and (right) in the range of 43–47°. It was calculated from the diffraction intensity that the content of perovskite phase for all the samples is more than 98%. Furthermore, calculated from the (0 0 2)/(2 0 0) peaks in the 2θ range of 43–47°, the modified PZT–PMSN, PZT–PMN, and PZT–PMN–PNN ceramic samples are in the tetragonal phase with tetragonality of c/a = 1.013, 1.010, 1.012, respectively, but the modified PZT–PMN–PZN and modified PZT–PMN–PNN ceramic samples are near the position of morphotropic phase boundary (MPB) with $c/a \sim 1$. In comparison with different doping conditions, it can be concluded that the ZnO and SnO_2 dopants diffuse into the structural lattice of PZT–PMN–PNN ceramics after sintering processing, which reduces the lattice tetragonal distortion towards the MPB.

Fig. 2 showed some typical SEM microstructure images of the fracture surface for the same samples as in Fig. 1. It is seen that the mechanical fracture behavior for the modified PZT–PMSN, PZT–PMN, modified PZT–PMN–PZN and modified PZT–PMN–PNN ceramics is predominantly transgranular, but the mixed mode of transgranular and intergranular for the PZT–PMN–PNN ceramics. As well known, piezoelectric ceramics is very much brittle and the intergranular fracture behavior is generally observed, which usually results from the weak mechanical bonding force of grain boundaries owing to impurities enriching or a thin layer of liquid phase existing on the grain boundaries [4,5,11]. Therefore, it is a substantial

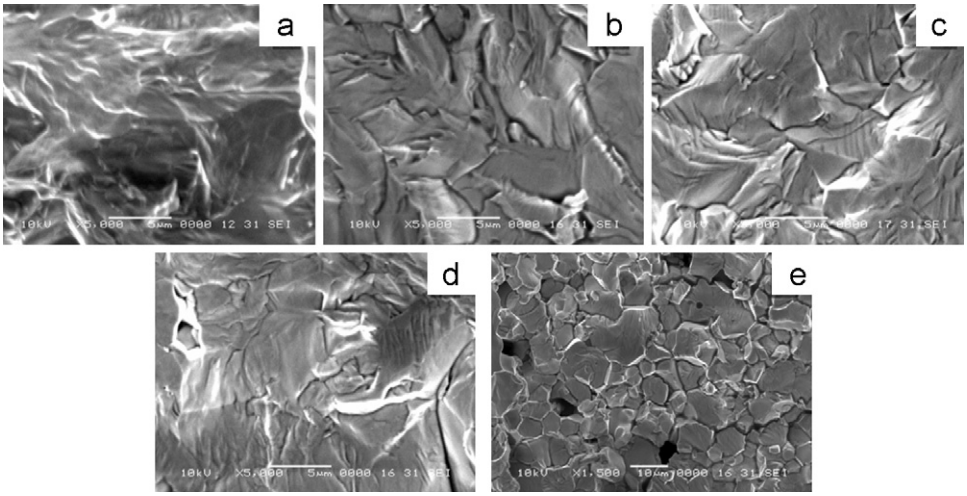

Fig. 2. SEM microstructure images of the fracture surface for the (a) modified PZT–PMSN, (b) PZT–PMN, (c) modified PZT–PMN–PZN, (d) modified PZT–PMN–PNN, and (e) PZT–PMN–PNN ceramic samples.

Table 1
The dielectric, ferroelectric and piezoelectric properties of the modified PZT–PMSN, PZT–PMN, modified PZT–PMN–PZN, PZT–PMN–PNN, and modified PZT–PMN–PNN ceramic samples.

Sample	ε_{33}^T	Tan δ (%)	P_r (μC/cm^2)	$E_c/-E_c$ (kV/cm)	d_{33} (pC/N)
Modified PZT–PMSN	1092	0.6	4.6	13.8/−7.4	226
PZT–PMN	2652	1.8	23.5	10.8/10.6	340
PZT–PMN–PNN	2374	1.9	22.6	8.6/−8.6	400
Modified–PZT–PMN–PNN	1843	1.9	19.2	8.6/−8.1	290
Modified PZT–PMN–PZN	2092	1.9	21.9	11.8/−11.8	267

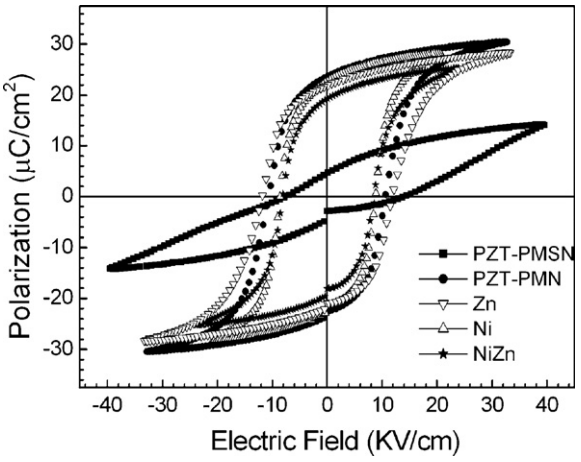

Fig. 3. Polarization–electric field hysteresis loops measured at room temperature for the same samples as in Fig. 1.

way to improve mechanical properties of piezoceramics through controlling character of grain boundaries to obtain transgranular fracture mode [2–5]. In our experiments, adding 1% ZnO + 0.5% SnO_2 into PZT–PMSN, 1.5% SiO_2 into PZT–PMN or 1% ZnO + 0.5% SnO_2 + 1.5% SiO_2 into PZT–PMN–PZN was found to change the fracture mode into transgranular, which is agreed with the previous observation on the $Pb(Zr_{0.58}Fe_{0.20}Nb_{0.20}\ Ti_{0.02})_{0.994}U_{0.006}O_3$ ceramics[8]. In contrast to the PZT–PMN–PNN piezoceramics with the mixed fracture mode of transgranular and intergranular, the addition of 1% ZnO + 0.5% SnO_2 made its fracture mode become predominant transgranular, as showed by Fig. 2(d) for the modified PZT–PMN–PNN piezoceramics. From Figs. 2(c) and (d), it can be seen that not only the doping element but also the main element of the piezoceramics set influence on the bonding force of grain boundaries. Related to the observed tetragonal distortion, it is reasonably concluded that the ZnO/SnO_2 additives diffuse into the PZT–PMN–PNN and PZT–PMN–PZN structural lattice and subsequently enhance the mechanical bonding forces of grain boundaries. To understand the underlying mechanism, a systematical characterization of the microstructure and characteristics of grain boundaries by high resolution transmission electron microscopy and selected area electron diffraction is required to be conducted.

Alternative to direct observations of grain boundaries, the dielectric, ferroelectric and piezoelectric properties of the modified PZT–PMSN, PZT–PMN, modified PZT–PMN–PZN, PZT–PMN–PNN, and modified PZT–PMN–PNN ceramic samples were measured at room temperature. In Fig. 3, the polarization–electric field hysteresis loops measured at frequency of 10 Hz were presented. The permanent polarization P_r and coercive field E_c were recorded and summarized in Table 1, together with the dielectric constant ε_{33}^T and dielectric loss tan δ, piezoelectric constant d_{33}. From Table 1, it was seen that the modified PZT–PMSN ceramic sample exhibits hard-type piezoelectric performance but the PZT–PMN, modified PZT–PMN–PZN, PZT–PMN–PNN, and modified PZT–PMN–PNN ceramics exhibit soft-type. It is of interest to note that adding ZnO/SnO_2 into PZT–PMN–PNN reduces the dielectric constant ε_{33}^T and piezoelectric constant d_{33}, which is agreed with the XRD observation of reduced tetragonal distortion. It is the diffusion of ZnO/SnO_2 into the lattice of PZT–PMN–PNN ceramic that reduces the tetragonal distortion and subsequently decreases the dielectric constant and piezoelectric constant, which can be understood well from the previous experimental investigations of the relationship between structural distortion and dielectric properties of PZT-based ceramics: the slight tetragonal distortion away from the MPB is beneficial to increase the dielectric constant and the maximum dielectric constant is usually observed at the position of $c/a \sim 1.01$ [14,15]. On the other hand, the Zn^{2+} ions in the ceramic lattice are also known to play a role of acceptor and would contribute to the reduction of dielectric constant and piezoelectric constant [16]. So far, the observations on the dielectric and piezoelectric properties of PZT–PMN–PNN and ZnO/SnO_2-doped PZT–PMN–PNN ceramics confirmed the conclusion from the SEM and XRD characterizations that the ZnO/SnO_2 additives were diffused into the structural lattice and resulted in those different mechanical and electrical performances.

4. Conclusion

The perovskite-type $(Pb_{0.95}Sr_{0.05})(Zr_{0.52}Ti_{0.48})O_3$–$Pb(Mn_{1/3}Sb_{2/3})O_3$–$Pb(Mn_{1/3}Nb_{2/3})O_3$ and $(Pb_{0.95}Sr_{0.04})(Zr_{1-x}Ti_x)O_3$–$Pb(Mg_{1/3}Nb_{2/3})O_3$ ceramics with various additives were prepared with conventional electroceramic processing. The modified PZT–PMSN, PZT–PMN, modified PZT–PMN–PZN, and modified PZT–PMN–PNN ceramics obtained here were observed predominantly to be transgranular fracture while the PZT–PMN–PNN ceramics exhibited mixed transgranular and intergranular. The fracture mode was observed associated not only with the doping elements but with the main elements of perovskite-type piezoelectrics as well. The mechanism of transgranular fracture mode observed here was understood by

the doping elements diffusion into the structural lattice of perovskite-type oxides, which enhanced the mechanical bonding force of grain boundaries, agreed with the experimental results of reduced tetragonality, dielectric constant and piezoelectric constant.

Acknowledgements

This work was partially supported by NSFC (50875181), NCET-07-0624, Shanghai Eastern Scholarship Program, and National Key Technology R & D Program of China (2009BAG12A04).

References

[1] A. Garg, T.C. Goel, Mechanical and electrical properties of PZT ceramics (Zr:Ti = 0.40:0.60) related to Nd^{3+} addition, Material Science and Engineering B 60 (1999) 128–132.
[2] J.H. Gong, Fracture Mechanics of Ceramics, Tsinghua University Publisher, Beijing, 2001.
[3] C.V. Verhoosel, M.A. Gutierrez, Modelling inter- and transgranular fracture in piezoelectric polycrystals, Engineering Fracture Mechanics 76 (2009) 742–760.
[4] E.R. Nielsen, E. Ringgaard, M. Kosec, Liquid-phase sintering of $Pb(Zr,Ti)O_3$ using $PbO–WO_3$ additive, Journal of the European Ceramic Society 22 (2002) 1847–1855.
[5] S. Jiansirisomboon, K. Songsiri, A. Watcharapasorn, T. Tunkasiri, Mechanical properties and crack growth behavior in poled ferroelectric PMN–PZT ceramics, Current Applied Physics 6 (2006) 299–302.
[6] S.J. Yoon, J.H. Moon, H.J. Kim, Piezoelectric and mechanical properties of $Pb(Zr_{0.52}Ti_{0.48})O_3–Pb(Y_{2/3}W_{1/3})O_3$ ceramics, Journal of Materials Science 32 (1997) 779–782.
[7] A. Garg, D.C. Agrawal, Effect of net PbO content on mechanical and electromechanical properties of lead zirconate titanate ceramics, Material Science and Engineering B 60 (1999) 46–50.
[8] H.T. Huang, P. Hing, Effect of SiO_2 additive on the mechanical and dielectric properties of PZFNTU ceramics, Ferroelectrics 229 (1999) 291–296.
[9] Y.D. Hou, M.K. Zhu, W. Hao, W. Bo, C.S. Tian, Y. Hui, Effects of atmospheric powder on microstructure and piezoelectric properties of PMZN–PZT quaternary ceramics, Journal of the European Ceramic Society 24 (2004) 3731–3737.
[10] F.X. Li, X.X. Yi, Z.Q. Cong, D.N. Fang, PZT nano-composites reinforced by small amount of MgO, Modern Physics Letters B 21 (2007) 1605–1610.
[11] R. Favaretto, D. Garcia, J.A. Eiras, Effects Of WO_3 on the microstructure and optical transmittance of PLZT ferroelectric ceramics, Journal of the European Ceramic Society 27 (2007) 4037–4040.
[12] L.H. Cao, X. Yao, Z. Xu, Dielectric and piezoelectric properties in fluoride-doped PMNT ceramics, Journal of Electroceramics 21 (2008) 593–596.
[13] S.X. Zhao, Q. Li, Y.C. Feng, C.W. Nan, Microstructure and dielectric properties of PMN–PT ceramics prepared by the molten salts method, Journal of Physics and Chemistry of Solids 70 (2009) 639–644.
[14] Y. (John) Yamashita, Y. Hosono, Material design of high-dielectric-constant and large-electromechanical-coupling-factor relaxor-based piezoelectric ceramics, Japanese Journal of Applied Physics 44 (2005) 7046–7049.
[15] G.C. Deng, Q.R. Yin, A.L. Ding, X.S. Zheng, W.X. Cheng, P.S. Qiu, High piezoelectric and dielectric properties of La-doped $0.3Pb(Zn_{1/3}Nb_{2/3})O_3–0.7Pb(Zr_xTi_{1-x})O_3$ ceramics near morphotropic phase boundary, Journal of the American Ceramic Society 88 (2005) 2310–2314.
[16] D. Berlincourt, Piezoelectric ceramic compositional development, Journal of the Acoustical Society of America 91 (1992) 3034–3040.